

Numerical simulation of internal (gravity) wave dynamics

Nils Wedi

European Centre for Medium Range Weather Forecasts (ECMWF), Reading, UK

Many thanks to P.K. Smolarkiewicz, A. Hollingsworth, T. Palmer,
A. Untch, M. Hortal, M. Miller, A. Tompkins, T. Jung, P. Bechtold and IBM

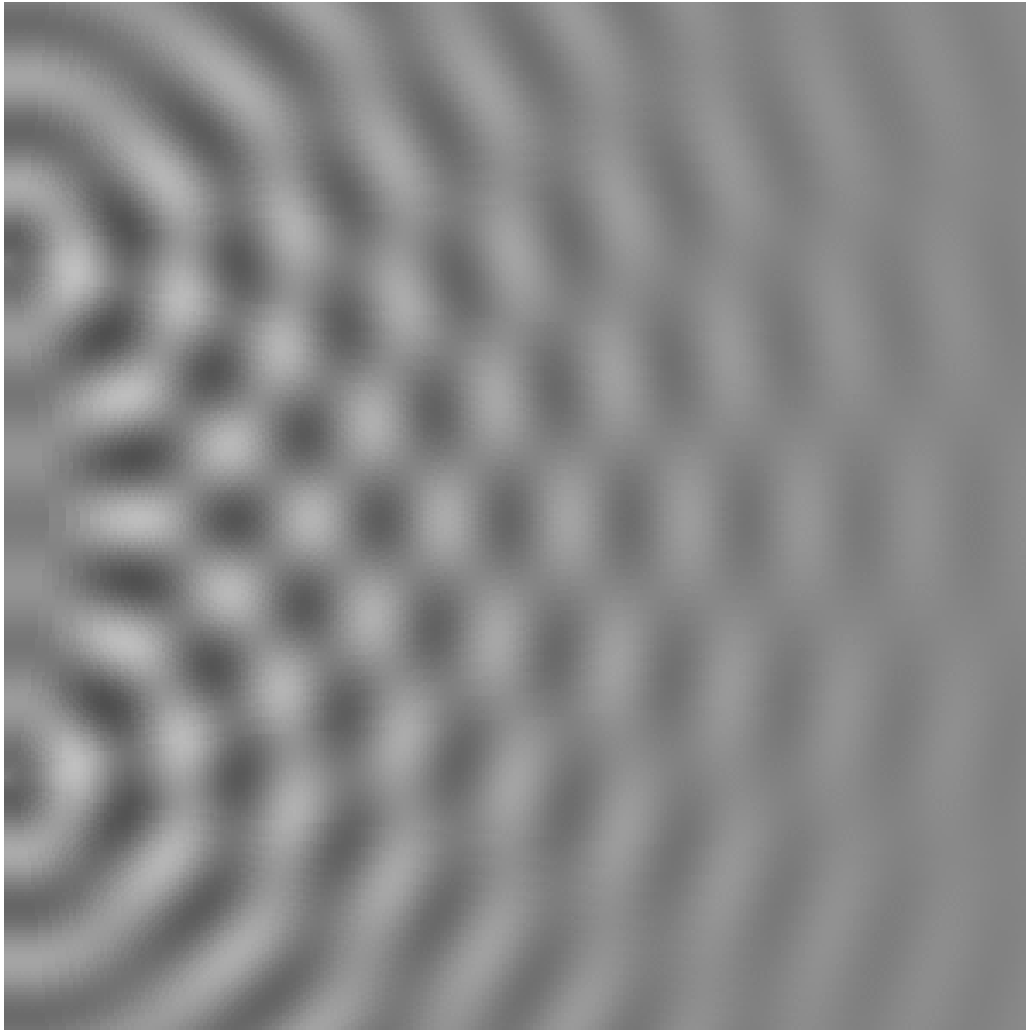


Outline

- Review aspects of observed and simulated internal (gravity) wave dynamics
- The laboratory experiment of Plumb and McEwan and its numerical equivalent
- Implications for the numerical realizability of internal (gravity) wave dynamics

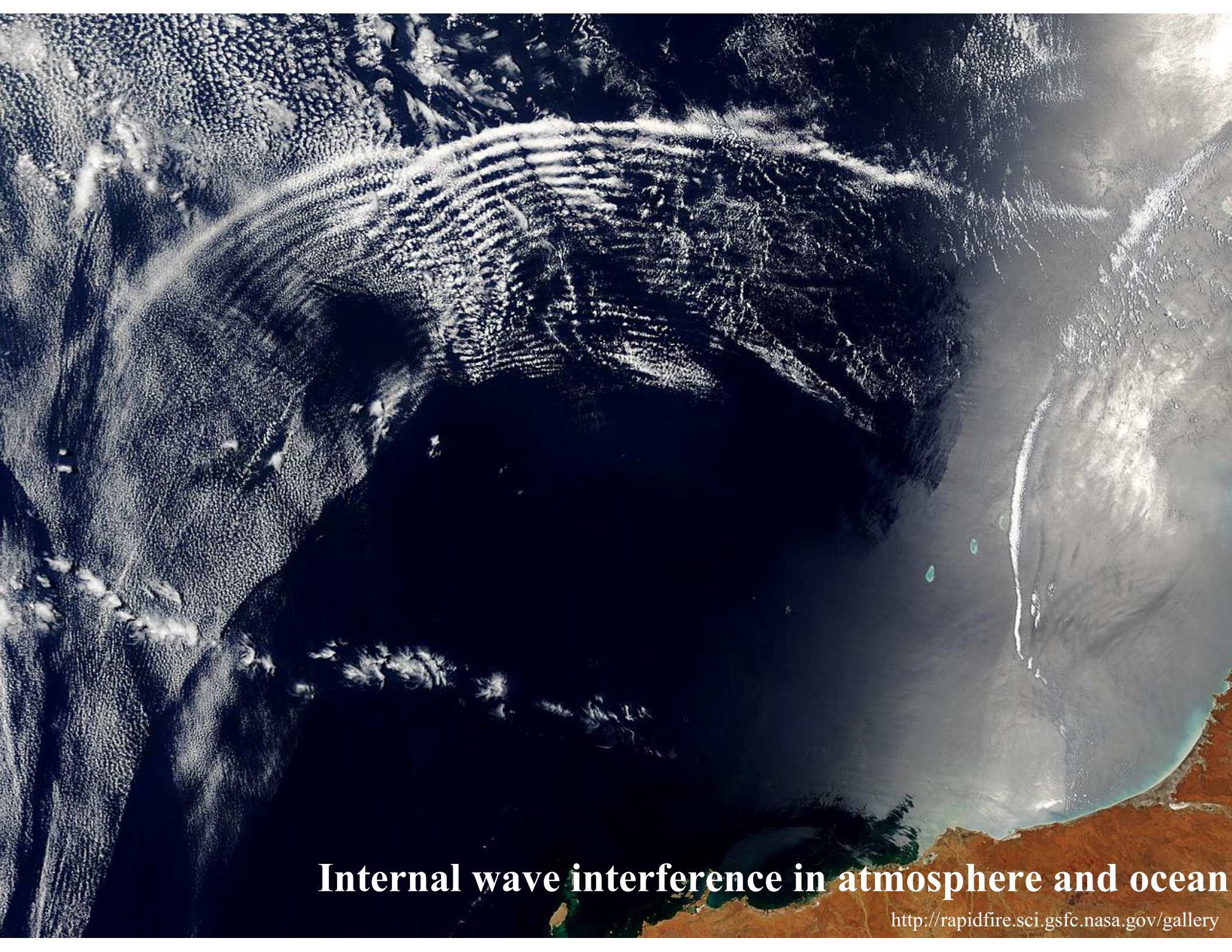


Wave interference



2 point source
interference pattern

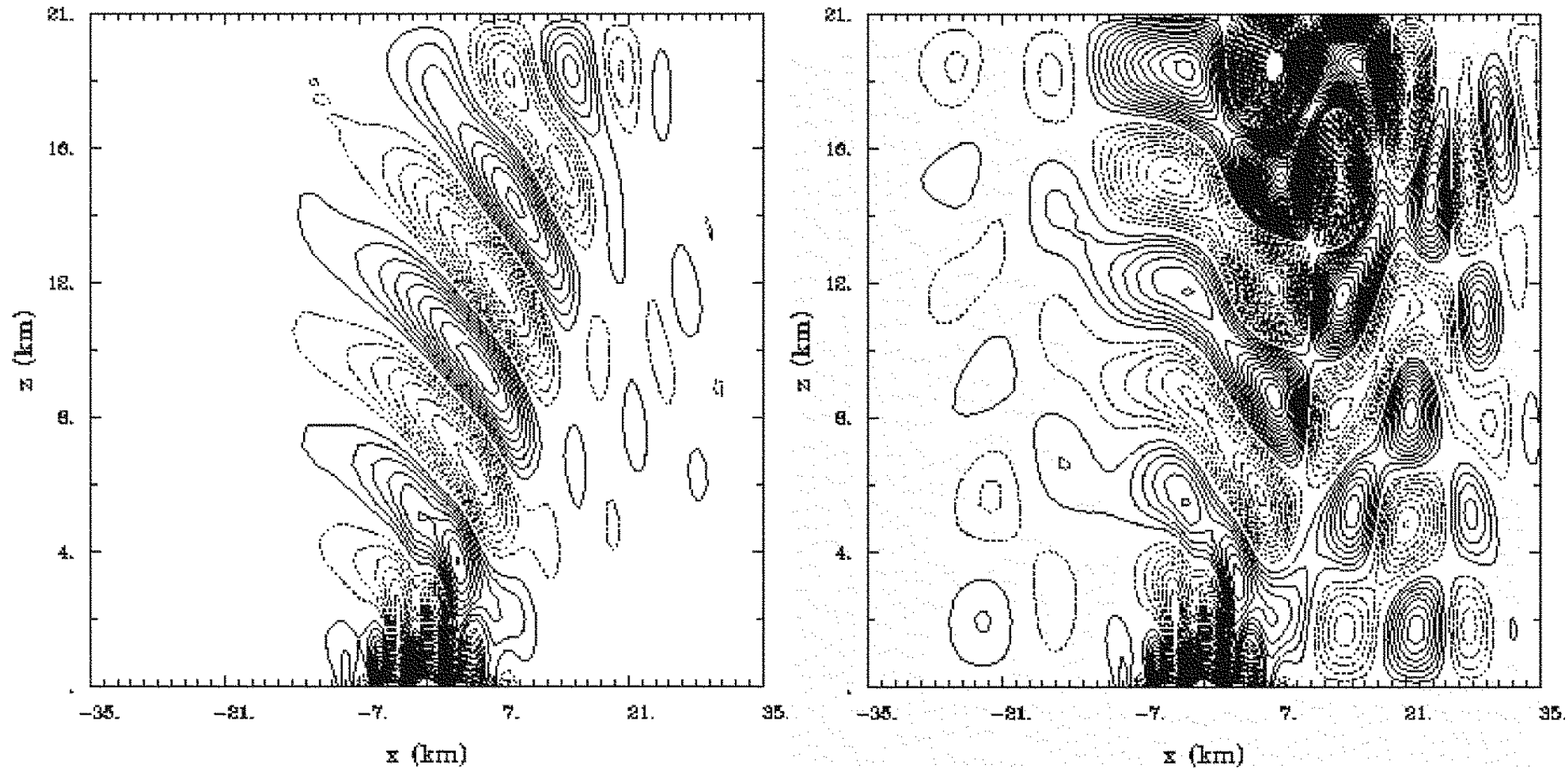




Internal wave interference in atmosphere and ocean

<http://rapidfire.sci.gsfc.nasa.gov/gallery>

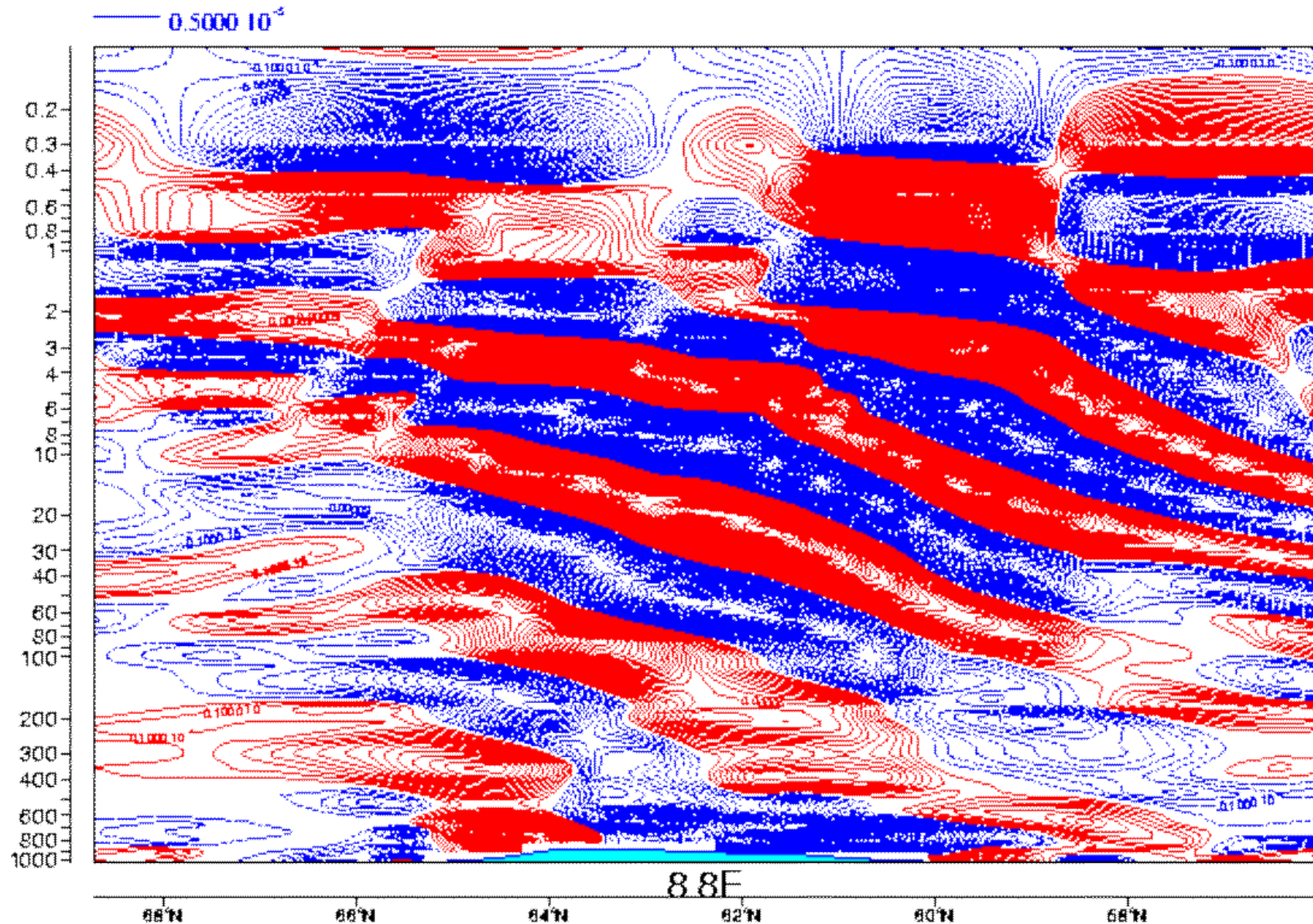
Example of gravity wave reflection (ambiguity: real or numerical ?)



Flow past Scandinavia

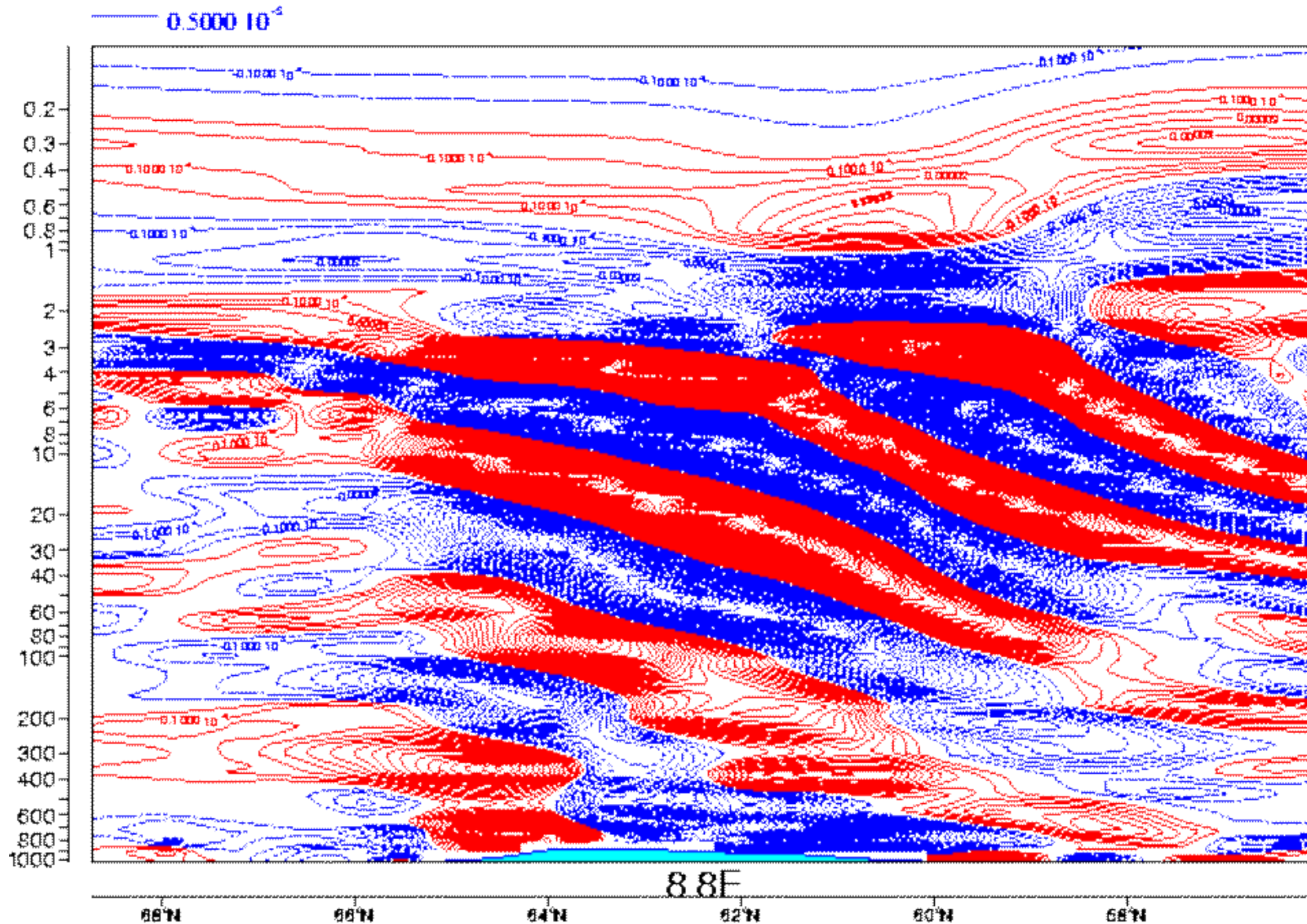
60h forecast 17/03/1998

divergence patterns with no absorbers aloft



Flow past Scandinavia 60h forecast 17/03/1998

divergence patterns in the operational configuration



Critical layers

Internal gravity waves in a stratified shear flow

459

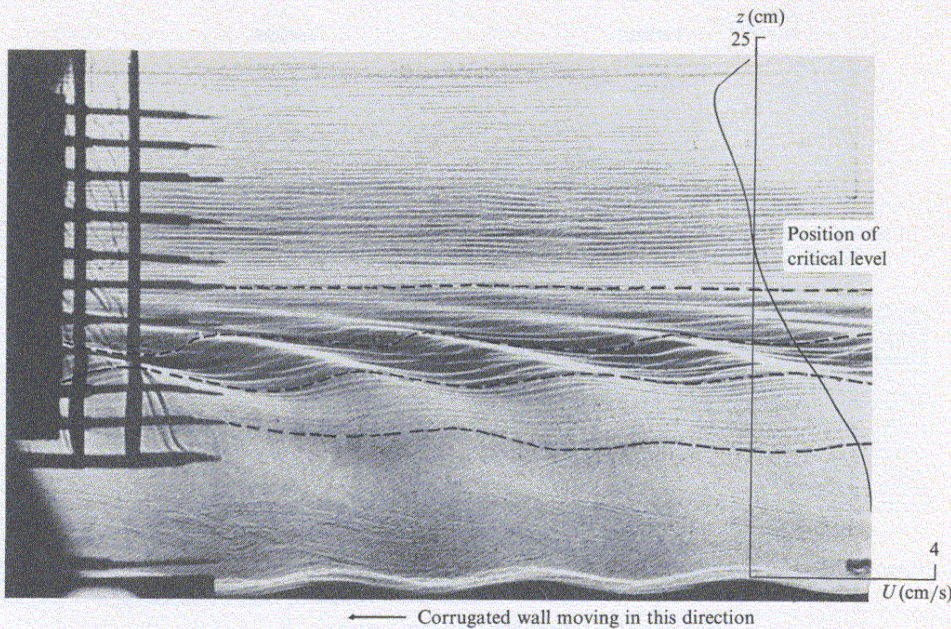


FIGURE 5. Shadowgraph image of wave field generated by 7.5 cm corrugated wall towed at 2.5 cm/s. Measured velocity profile (in coordinate system moving with corrugated wall) is shown superimposed on the photograph. Position of critical level noted by an arrow. Dotted lines have been superimposed on the photograph to accentuate the isopycnal displacements.

Internal gravity waves in a stratified shear flow

461

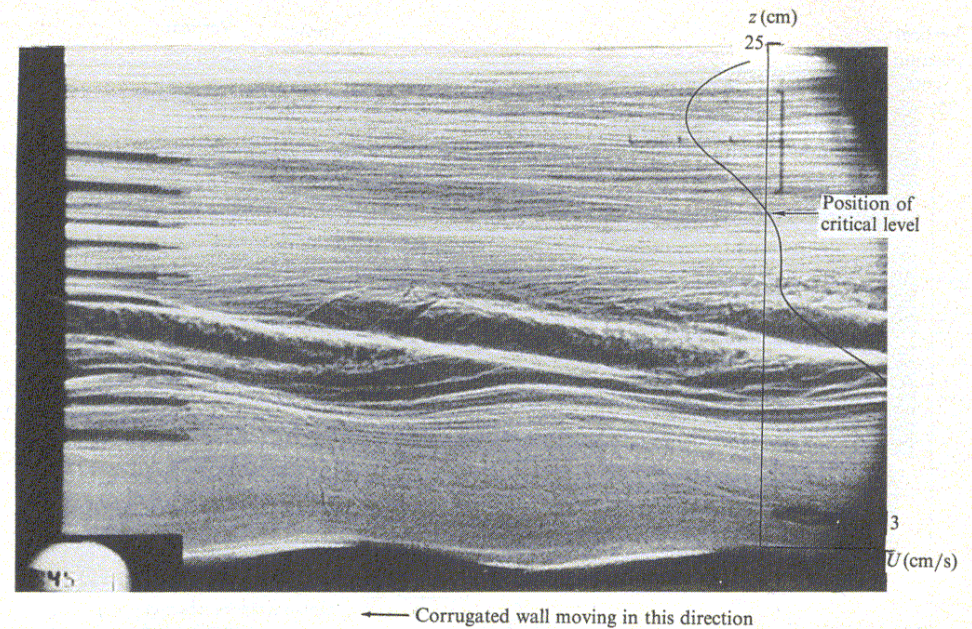


FIGURE 7. Shadowgraph of wave field generated by 15 cm corrugated wall towed at 3.88 cm/s. Measured velocity profile (in coordinate system moving with corrugated wall) is shown superimposed on the photograph. Position of critical level noted by an arrow.

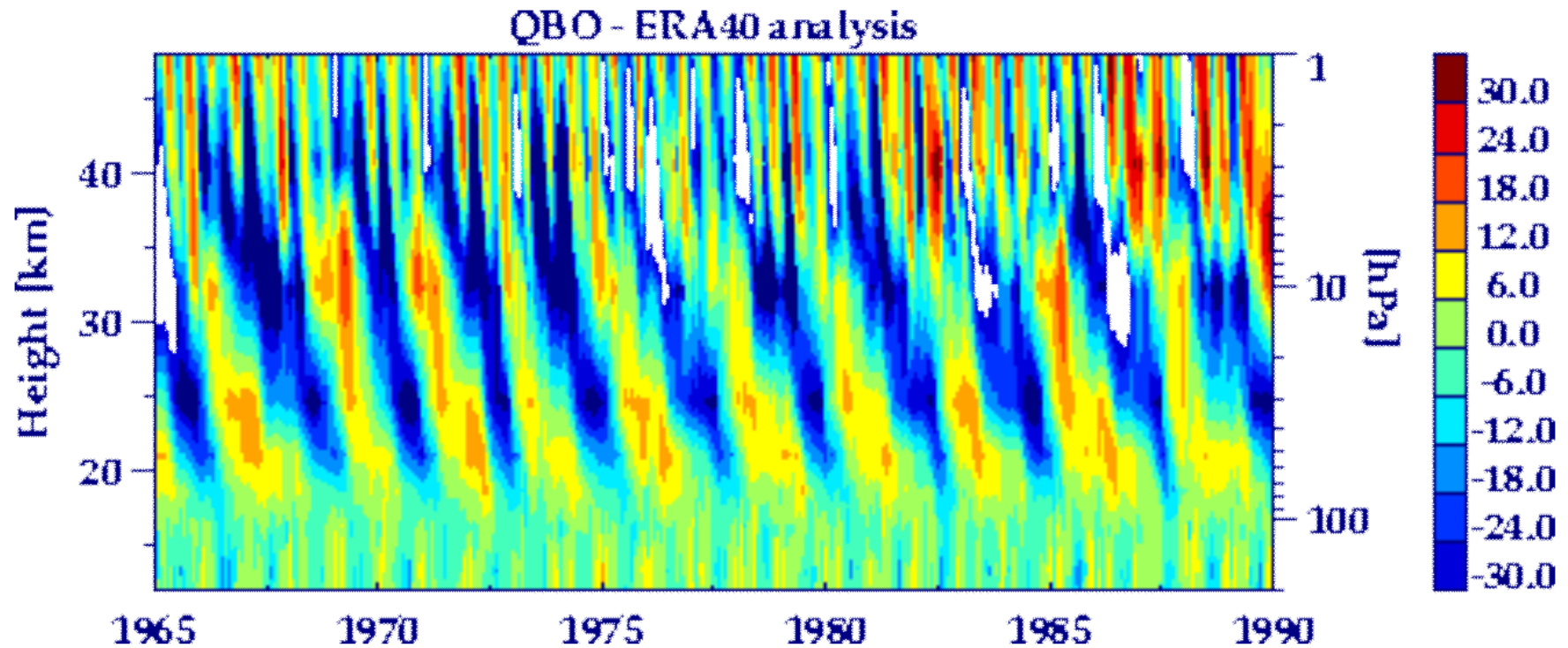
(Koop and McGee, 1986)



Wave breaking



Wave-mean flow interaction



Approximate solutions (WKB)

(Bretherton, 1966; Grimshaw, 1972,1974,1975; Baines 1995)

$$(\omega(z, t) - \underline{kU(z, t)})^2 = \frac{N^2 k^2}{k^2 + \underline{m^2(z, t)}}$$

$$\frac{\partial U}{\partial t} = \boxed{-\frac{\partial \overline{u'w'^x}}{\partial z}} + \nu \frac{\partial^2 U}{\partial z^2}$$

$$\frac{\partial}{\partial t} \mathcal{A}(z, t) + \frac{\partial}{\partial z} c_{gz} \underline{\mathcal{A}(z, t)} = -(\nu + \kappa)(k^2 + m^2(z, t)) \mathcal{A}(z, t)$$

$$\mathcal{A} := \frac{\varepsilon}{\omega - Uk}$$

$$\frac{k}{\rho_0} \frac{\partial}{\partial z} c_{gz} \mathcal{A} = \frac{\partial \overline{u'w'^x}}{\partial z}$$

$$c_{gz} := \frac{\partial \omega}{\partial m}$$



Method

- Employ a direct numerical simulation (DNS) of the QBO analogue to understand in detail the mechanism leading to the oscillation in the laboratory
- Investigate numerical and parametric sensitivities of the arising oscillation to draw conclusions on the numerical realizability of zonal mean flow oscillations



The laboratory experiment of Plumb and McEwan

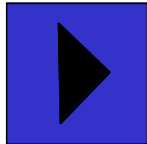
http://www.gfd-dennou.org/library/gfd_exp/exp_e/index.htm

- The principal mechanism of the QBO was demonstrated in the laboratory experiment of *Plumb and McEwan (1978)* and later repeated at the University of Kyoto.



The laboratory experiment of Plumb and McEwan

Animation:



[A short movie of the original laboratory experiment](#)

Plumb and McEwan, J. Atmos. Sci. 35 1827-1839 (1978)



The generalized time-dependent coordinate transformation

$$\bar{x}^1 \equiv \bar{x} = E(x, y, t)$$

*Wedi and Smolarkiewicz,
J. Comput. Phys 193(1) (2004) 1-20*

$$\bar{x}^2 \equiv \bar{y} = D(x, y, t)$$

$$\bar{x}^3 \equiv \bar{z} = C(x, y, z, t) = C(\xi)$$

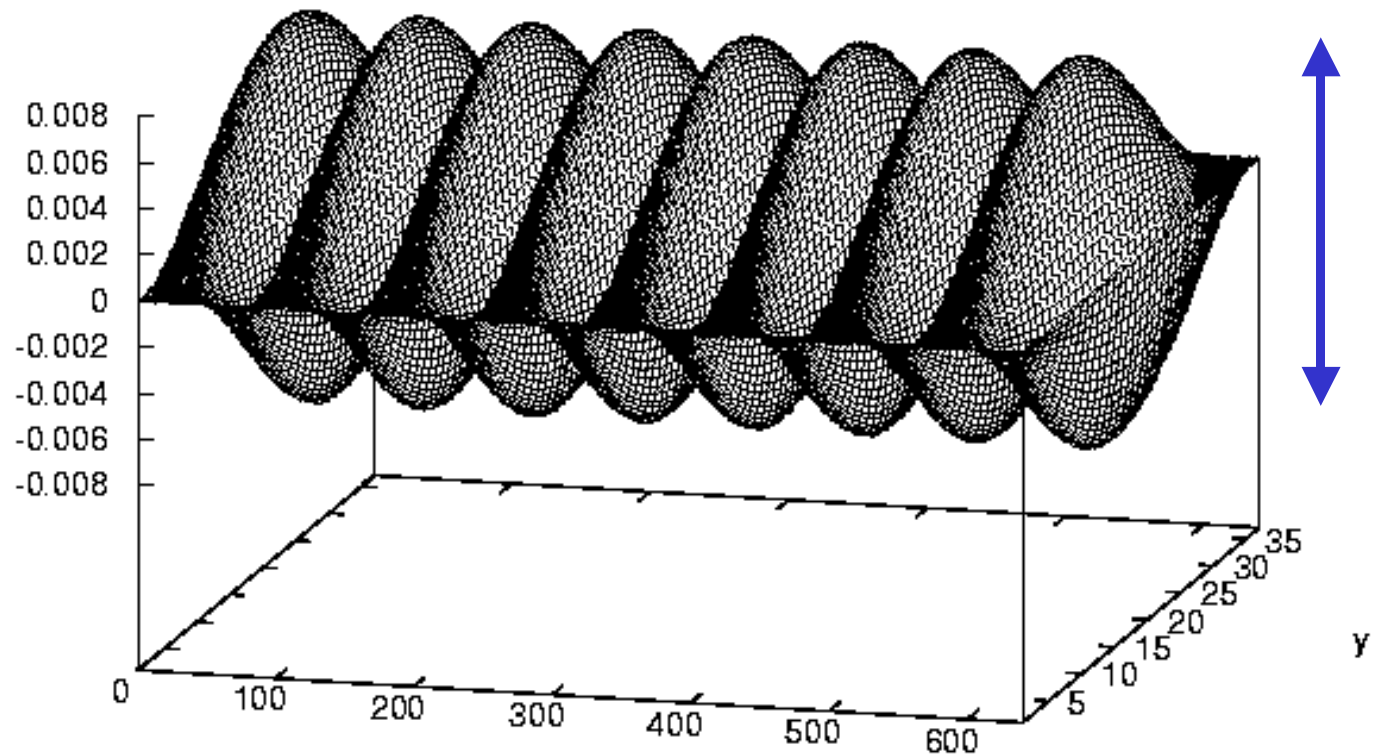
$$\xi = \xi(x, y, z, t) := H_0 \frac{z - z_s(x, y, t)}{H(x, y, t) - z_s(x, y, t)}$$

Time dependent boundaries



Oscillating membrane

$$H(x, y, t) \text{ or } z_s(x, y, t)$$



$$H(x, y, t) = H_0 - z_s(x, y, t).$$

$$z_s(x, y, t) = \epsilon \sin\left(\frac{\pi}{L_y} y\right) \sin\left(\frac{2\pi s}{L_x} x\right) \sin(\omega_0 t)$$



Boussinesq equations

$$\nabla \cdot (\rho_b \mathbf{v}) = 0,$$

$$\frac{D\mathbf{v}}{Dt} = -\nabla\pi' + \mathbf{g}\frac{\rho'}{\rho_b} + \frac{1}{\rho_b}\nabla \cdot \boldsymbol{\tau},$$

$$\frac{D\rho'}{Dt} = -\mathbf{v} \cdot \nabla\rho_e + \kappa\nabla^2\rho'.$$



Generalized coordinate equations

$$\frac{\partial(\rho^* \overline{v}^{s^k})}{\partial \overline{x}^k} = 0 ,$$

$$\frac{dv^j}{d\bar{t}} = - \tilde{G}_{ij}^k \frac{\partial \pi'}{\partial \overline{x}^k} - g \frac{\rho'}{\rho_b} \delta_3^j + F^j + \mathcal{V}^j ,$$

$$\frac{d\rho'}{d\bar{t}} = - \overline{v}^{s^k} \frac{\partial \rho_e}{\partial \overline{x}^k} + \mathcal{H} .$$

Strong conservation formulation ! (*T. Clark, 1977*)



Explanations ...

Using:

Jacobian of the transformation

$$\rho^* := \rho_b \bar{G},$$

Transformation coefficients

$$\tilde{G}_j^k := \sqrt{g^{jj}} (\partial \bar{x}^k / \partial x^j),$$

Contravariant velocity

$$\bar{v}^{*k} := d\bar{x}^k / d\bar{t} := \dot{\bar{x}}^k,$$

Solenoidal velocity

$$\bar{v}^{sk} := \bar{v}^{*k} - \frac{\partial \bar{x}^k}{\partial t},$$

Physical velocity

$$\bar{v}^{sk} = \tilde{G}_j^n v^n$$



Numerical Approximation

Compact conservation-law form:

$$\frac{\partial \rho^* \psi}{\partial \bar{t}} + \bar{\nabla} \cdot (\rho^* \bar{\mathbf{v}}^* \psi) = \rho^* R$$

Lagrangian Form:

$$\frac{d\psi}{d\bar{t}} = R$$

$$\Rightarrow \psi_{\mathbf{i}}^{n+1} = LE_{\mathbf{i}}(\tilde{\psi}) + 0.5\Delta t R_{\mathbf{i}}^{n+1}$$



Numerical Approximation

with

$$\tilde{\psi} := \psi^n + 0.5\Delta t R^n$$

*LE, flux-form Eulerian or Semi-Lagrangian formulation using MPDATA advection schemes
Smolarkiewicz and Margolin (JCP, 1998)*

$$\nabla \cdot \rho^* \bar{\mathbf{v}}^s = 0$$

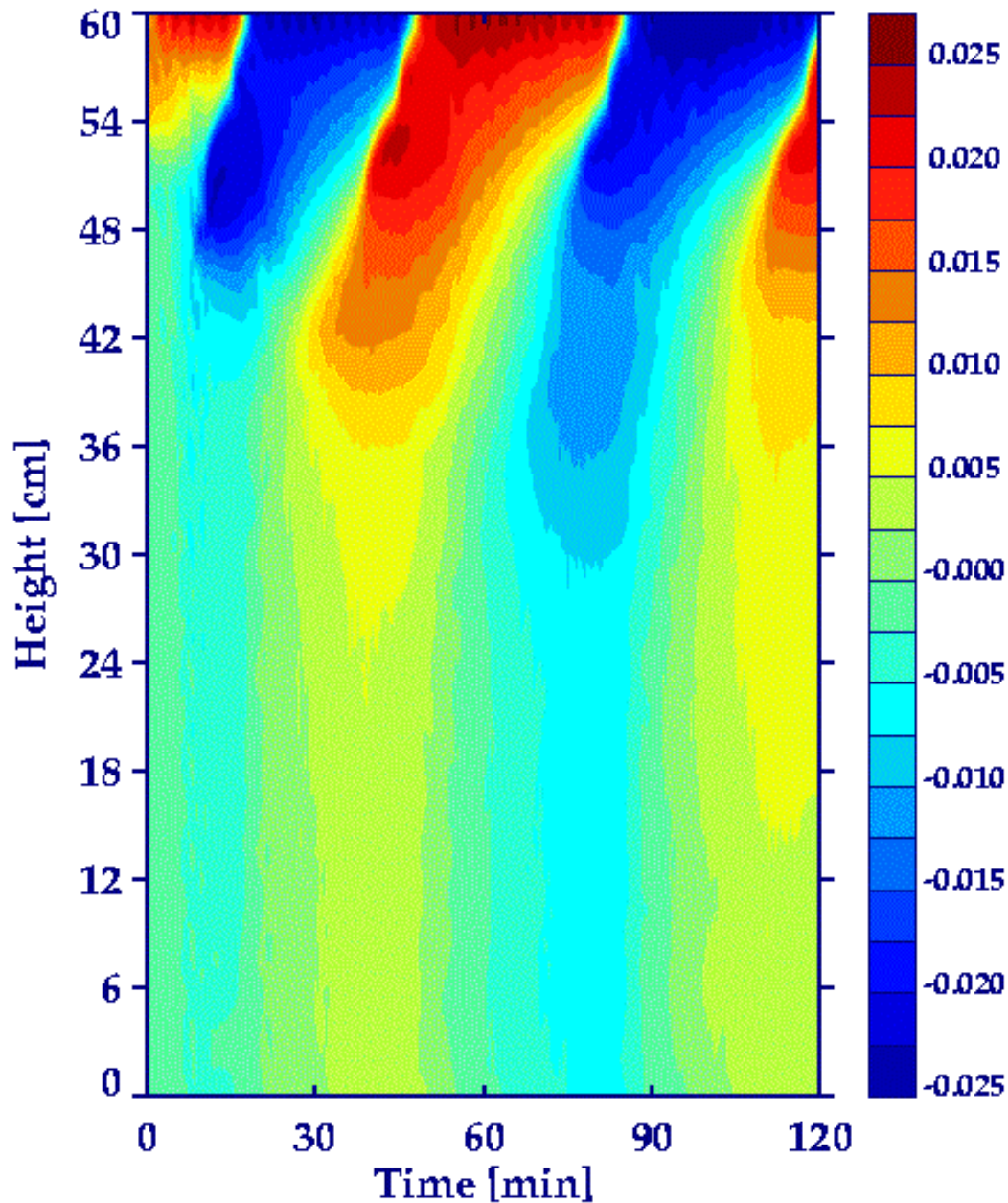
$$\Rightarrow -\frac{\Delta t}{\rho^*} \sum_{i=1}^3 \frac{\partial}{\partial \bar{x}^i} \left[\rho^* \varepsilon \left(v^i - \sum_{j=1}^3 c^{ij} \frac{\partial \pi'}{\partial \bar{x}^j} \right) \right] = 0$$

with

Prusa and Smolarkiewicz (JCP, 2003)

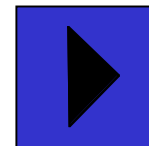
$\bar{\mathbf{v}}^* \cdot \mathbf{n}$ specified and/or periodic boundaries



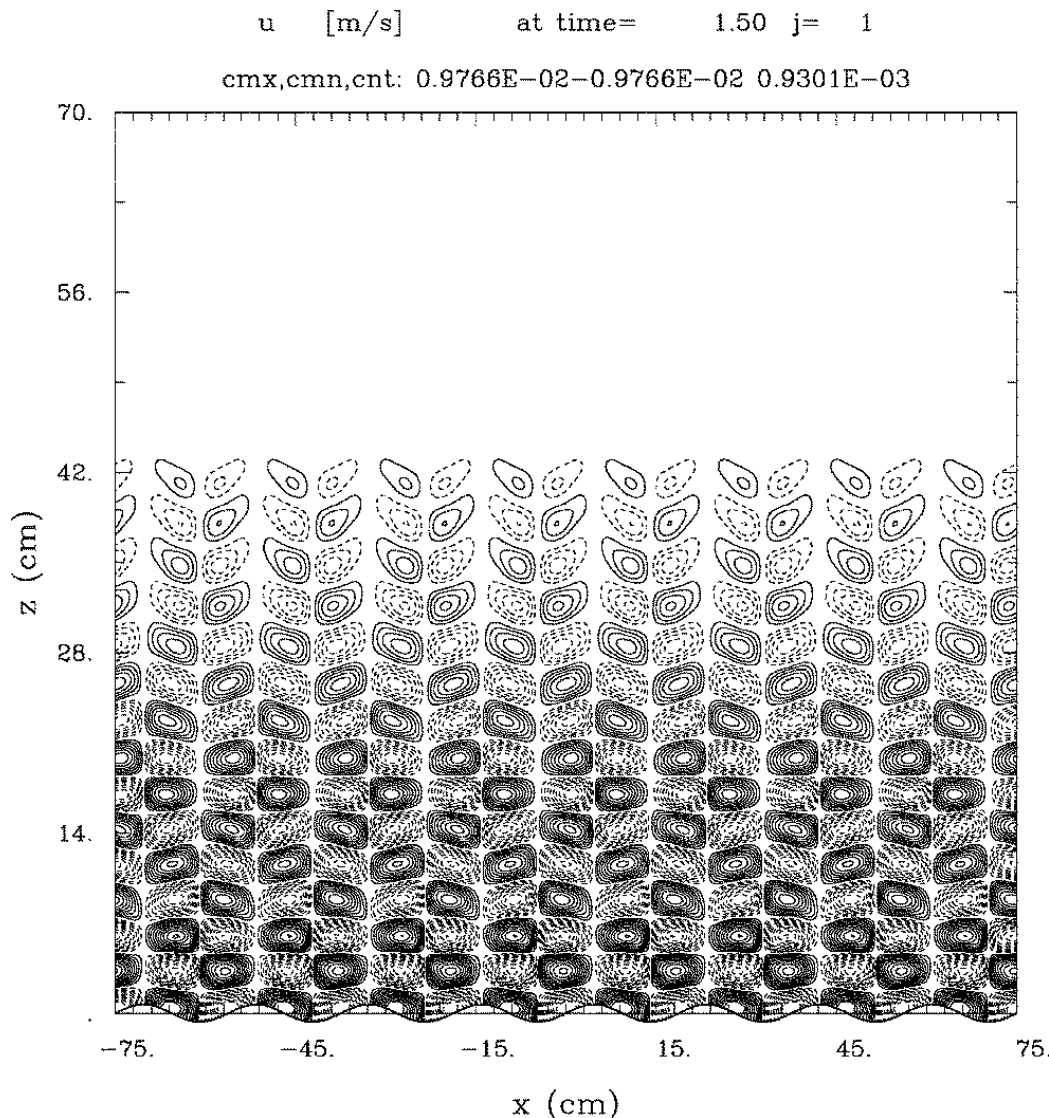


Time – height cross
section of the mean
flow U
in a 3D simulation

Animation



What happens then really in the laboratory experiment ?

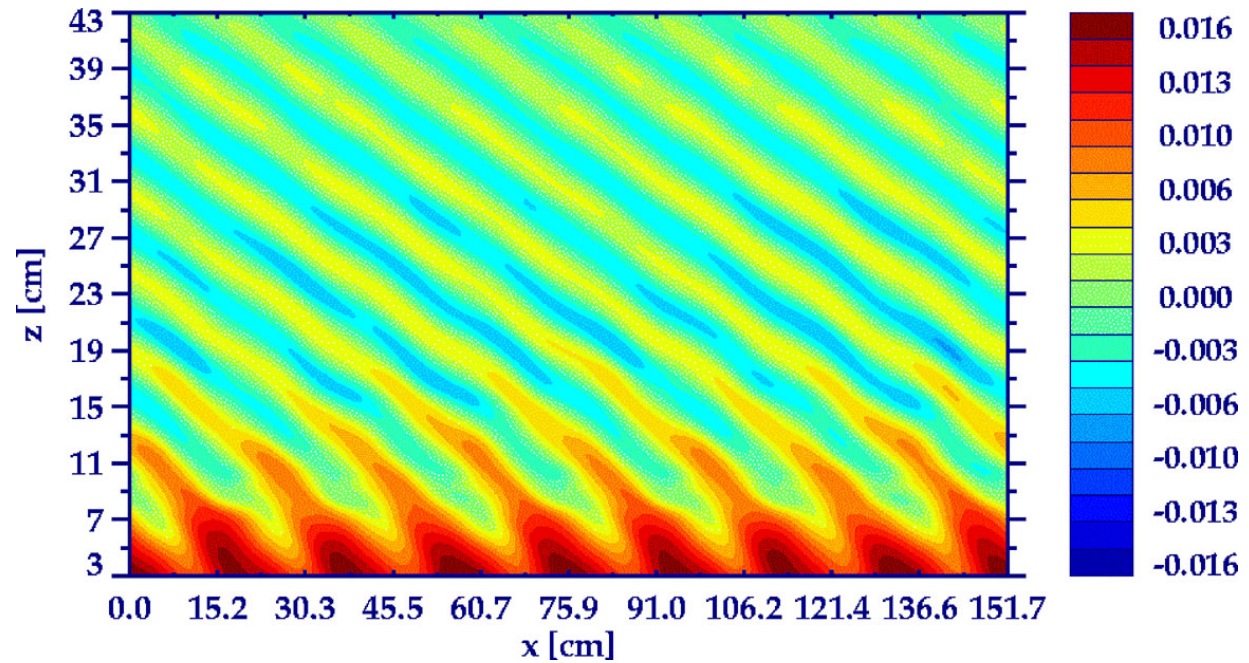


- Recall: a standing wave is equivalent to two travelling waves one left and one right with wave-number $k = 8$, $k = -8$)
- The observed frequency of the waves equals the forcing frequency $\omega_0 = 0.43\text{s}^{-1}$

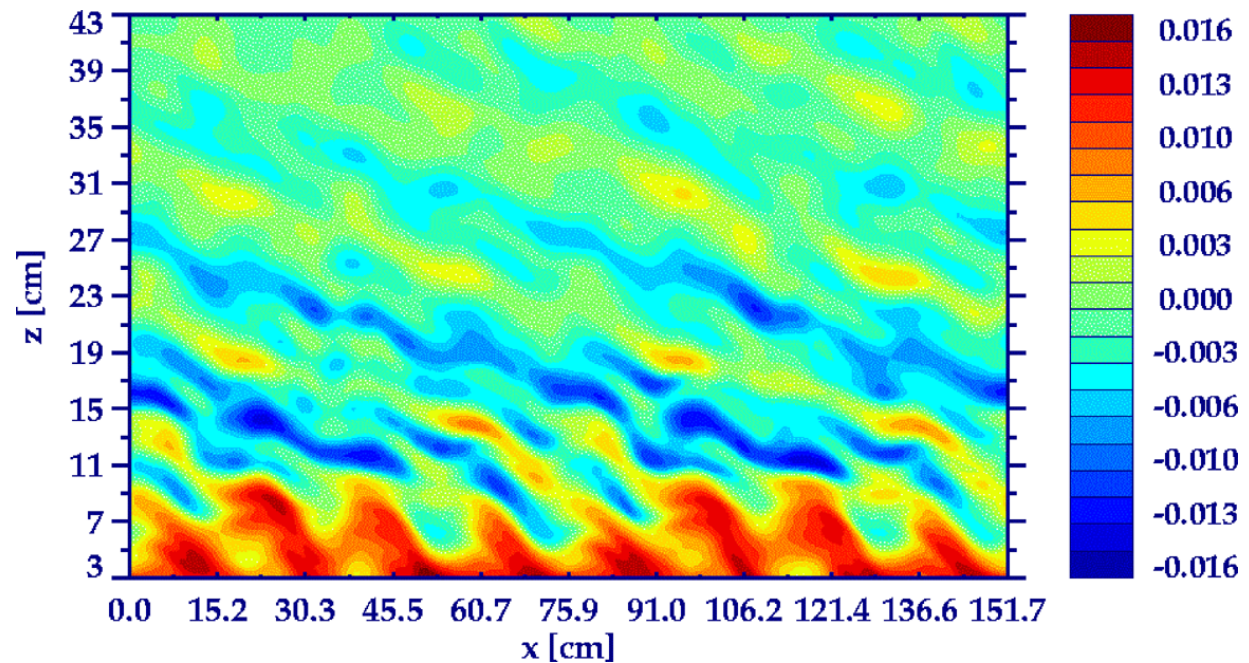


Wave interference

T=24min



T=26min



The mean flow becomes critical...

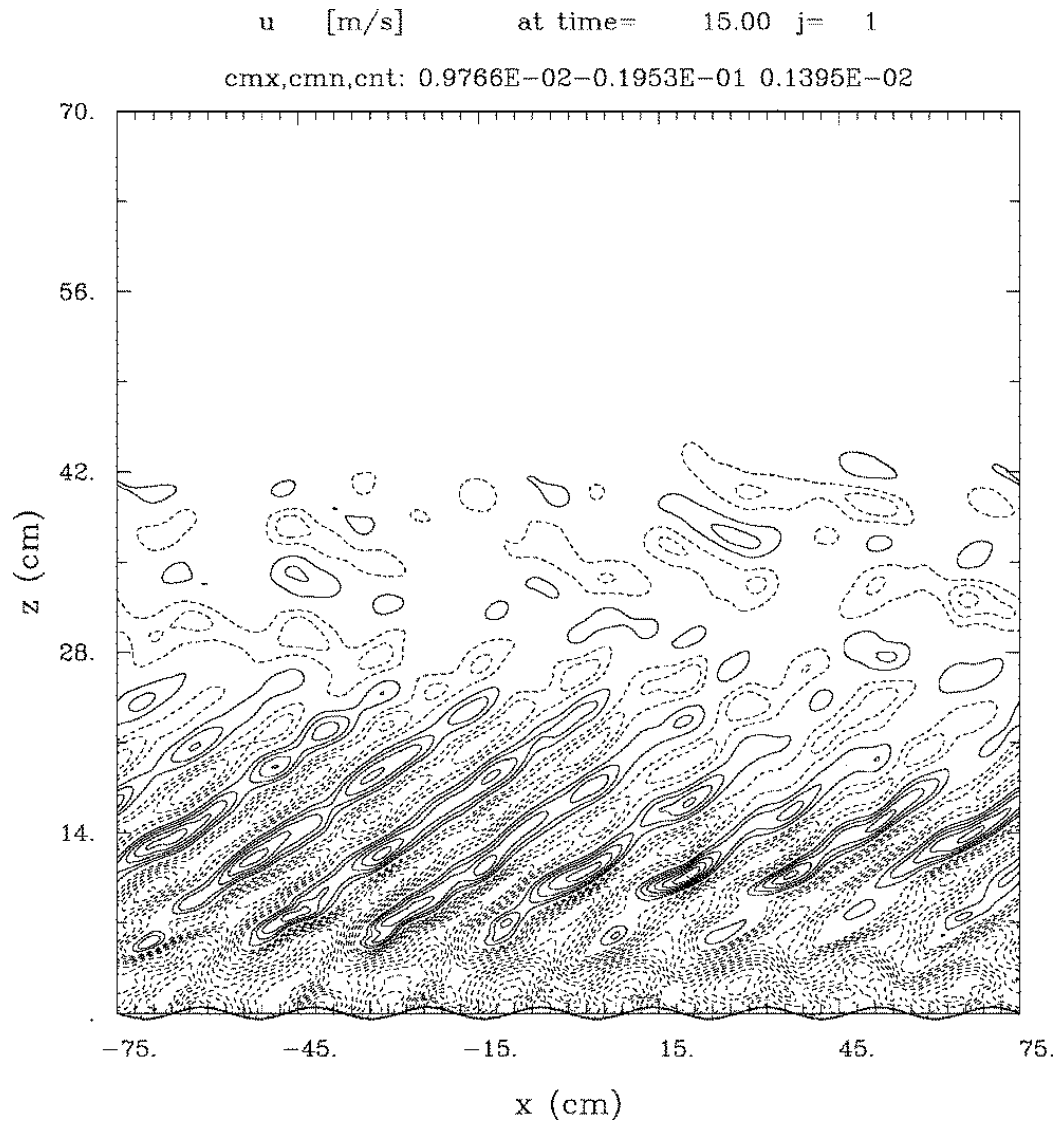
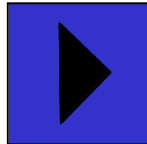
- The dispersion relation for linearized inviscid Boussinesq flow exhibits a singularity when the magnitude of the phase speed of a wave equals the mean flow speed and the wave travels in the same direction as the mean flow.
- In viscous nonlinear flow there is a wave momentum flux contributing to a mean flow change in some region near this point

$$U_{crit} = \frac{\omega_0}{(2\pi s / L_x)}$$



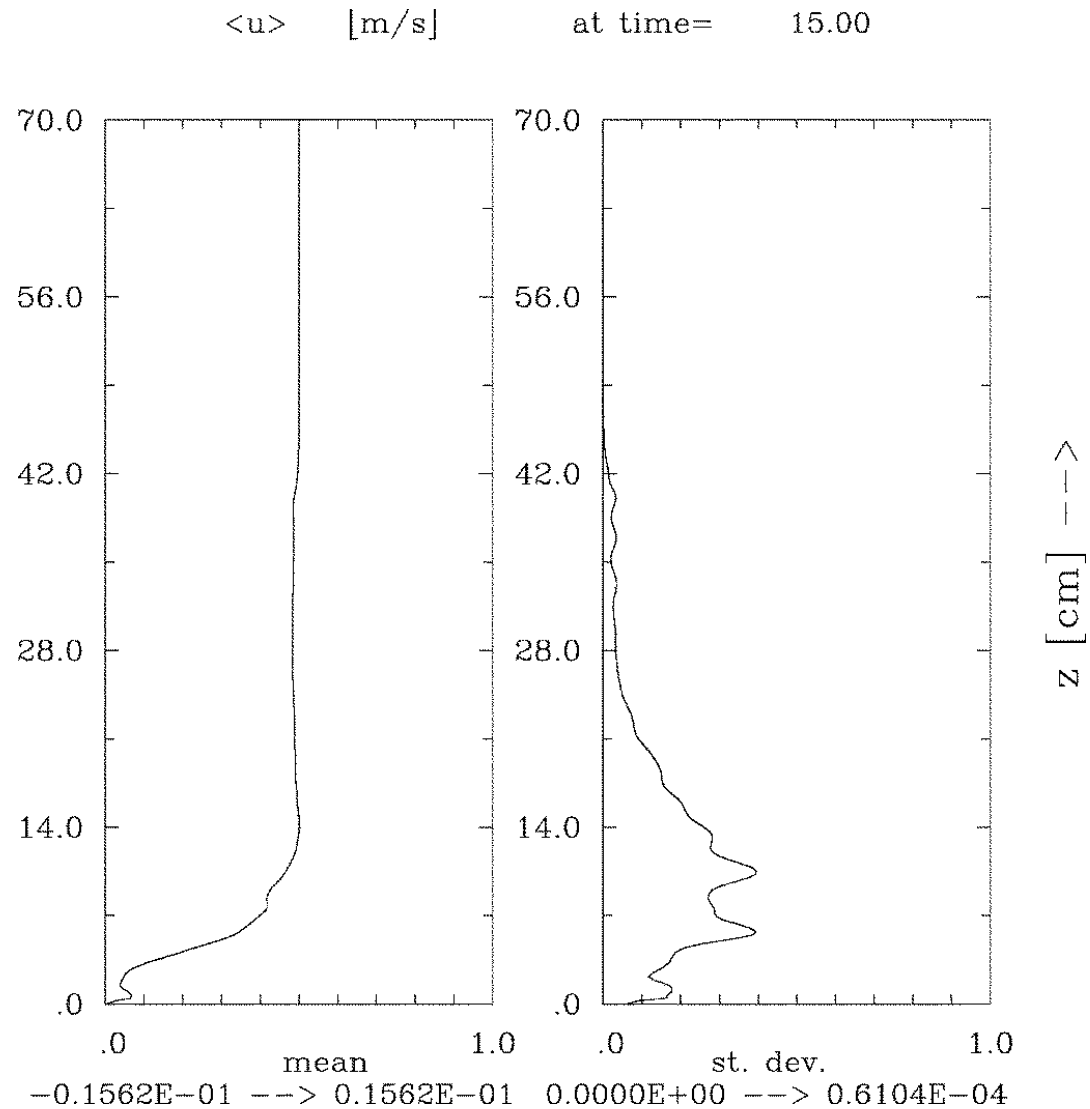
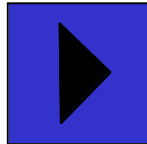
XZ-cross section u

Animation:



Mean flow profile U

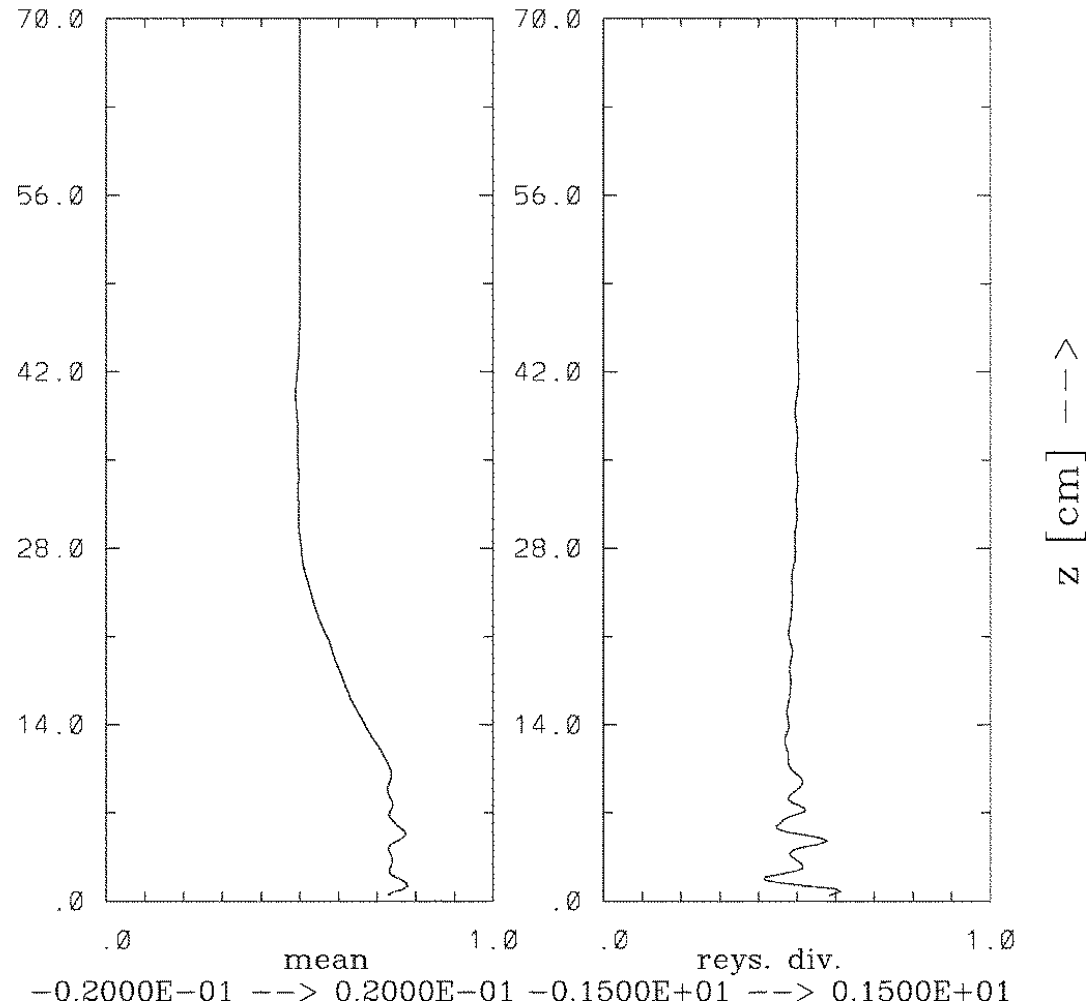
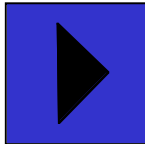
Animation:



wave momentum flux and its divergence

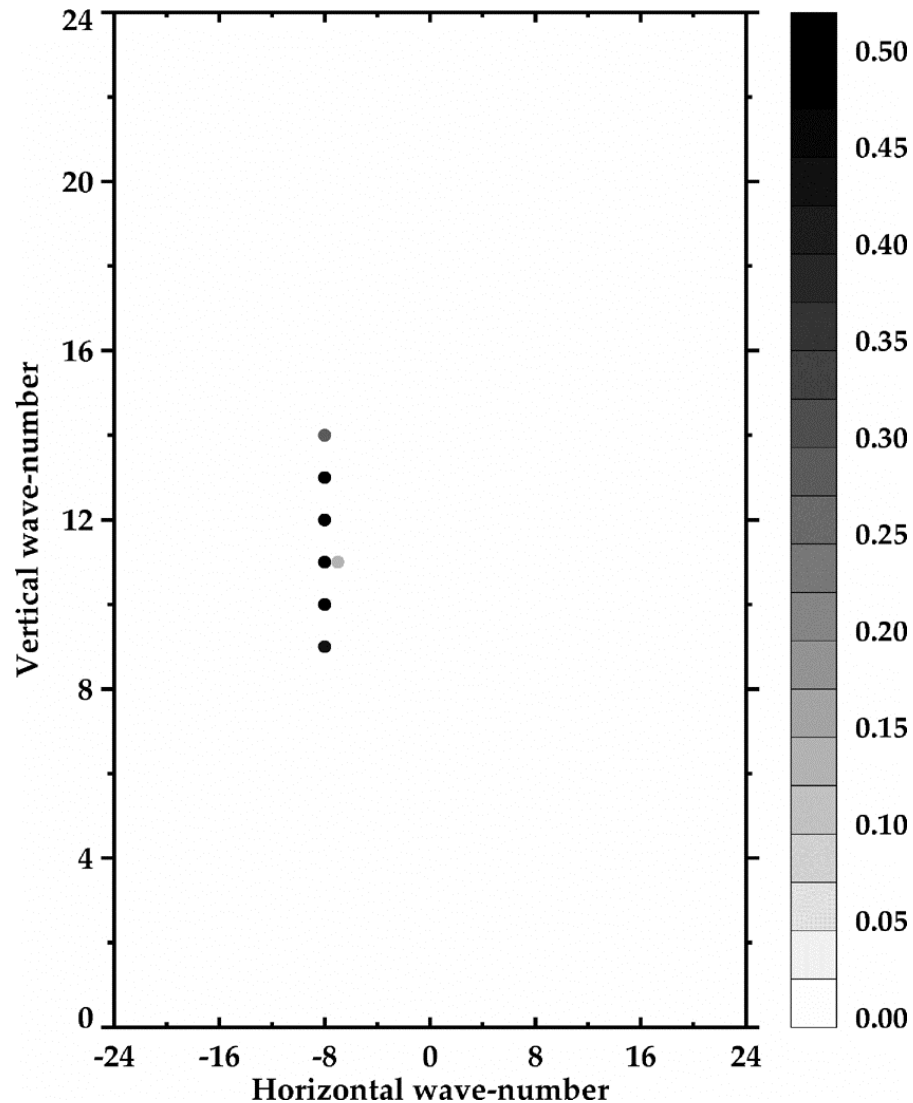
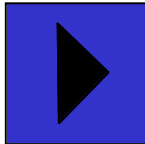
$\langle \rho \cdot (u - \langle u \rangle) \cdot (w - \langle w \rangle) \rangle$ at time = 15.00

Animation:



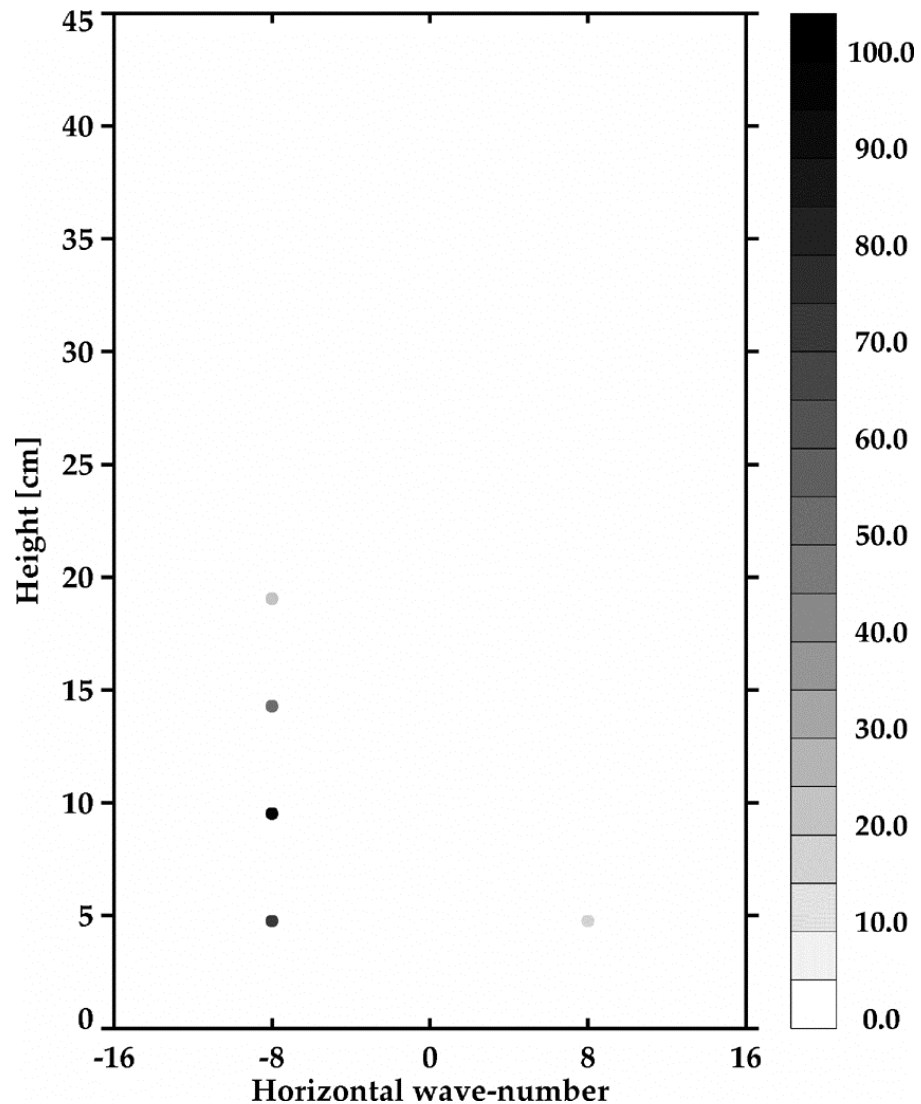
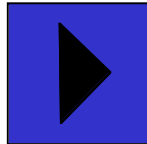
Spectral analysis: Horizontal – Vertical wave number

Animation:

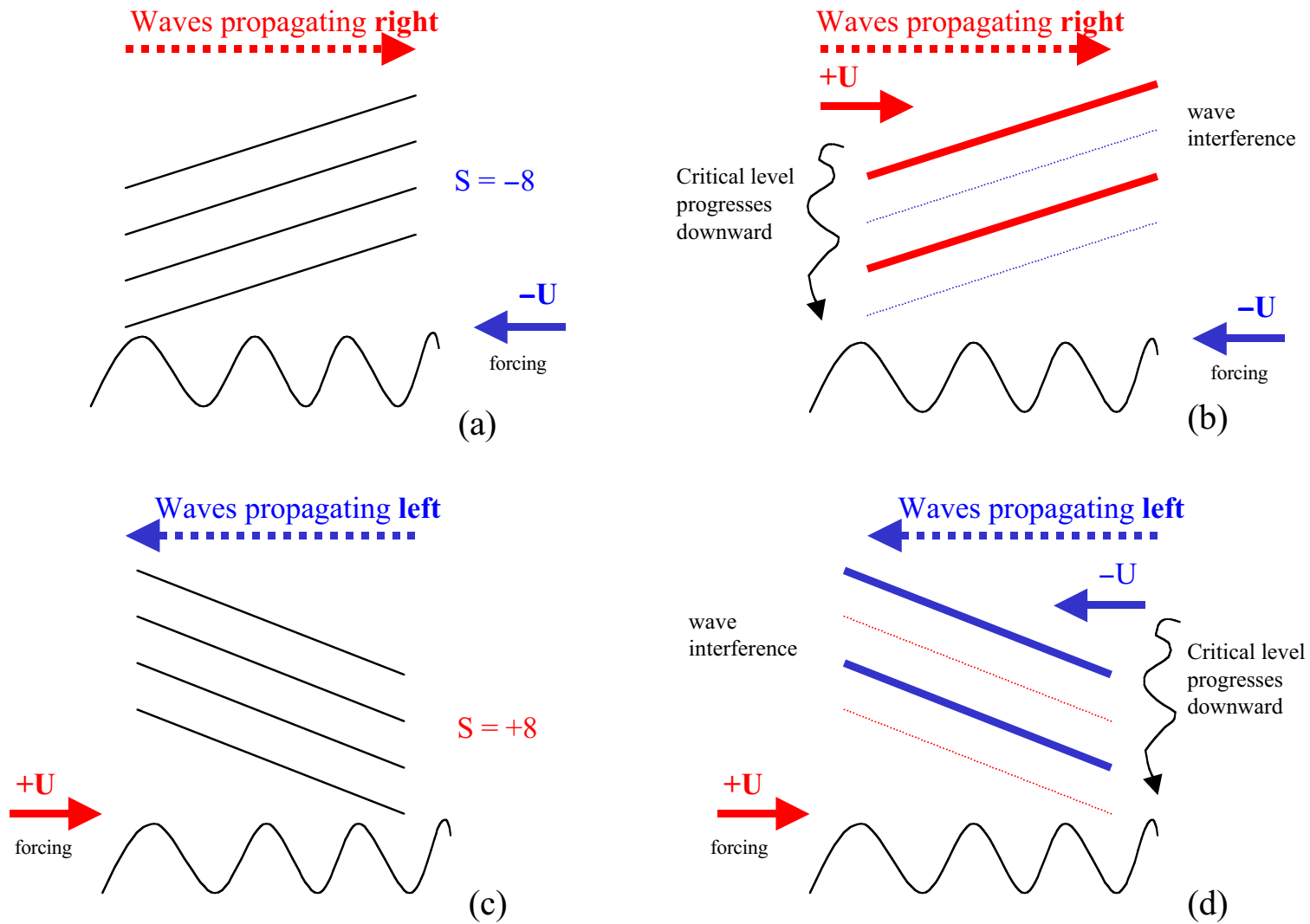


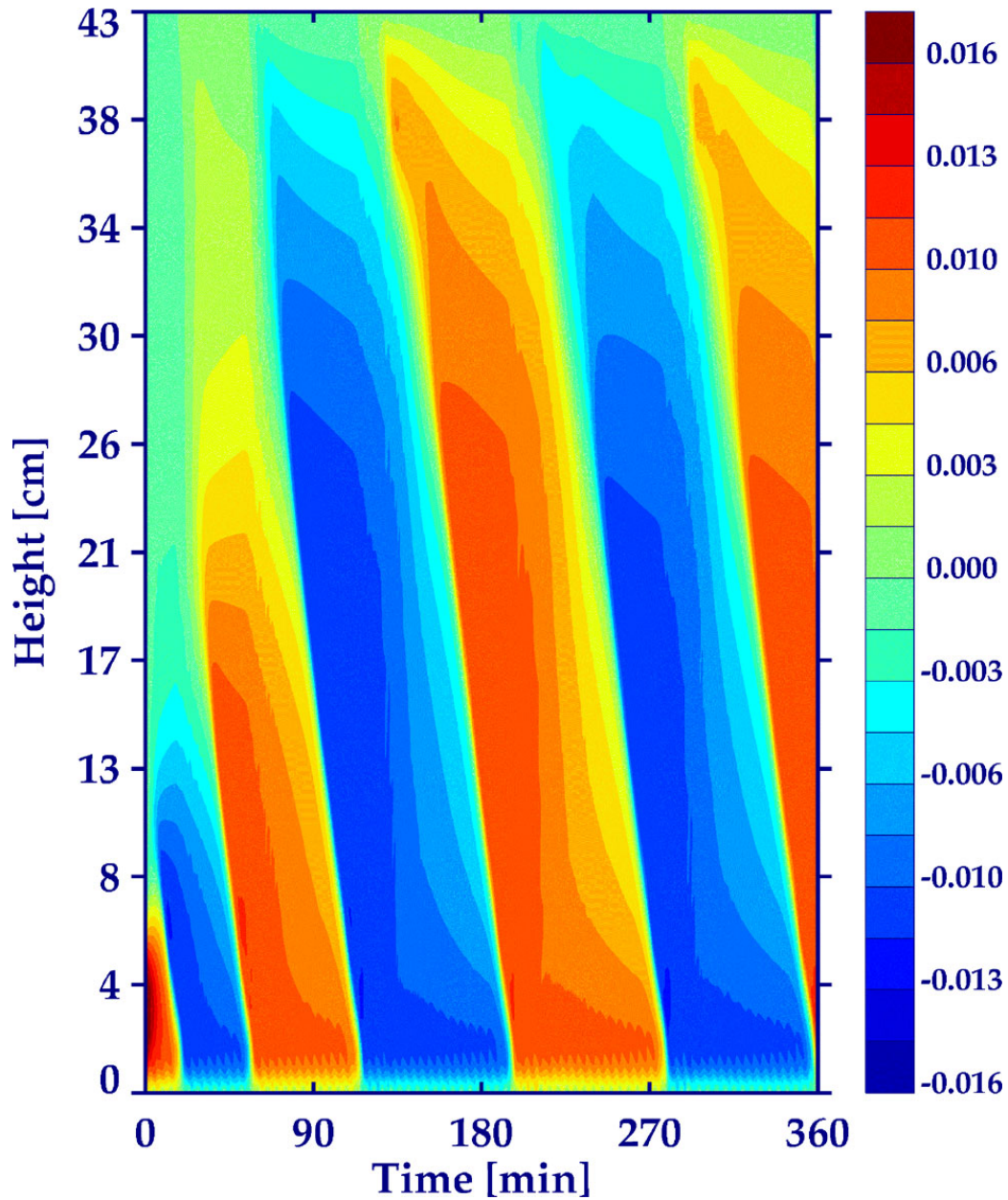
Horizontal wave number at different heights

Animation:

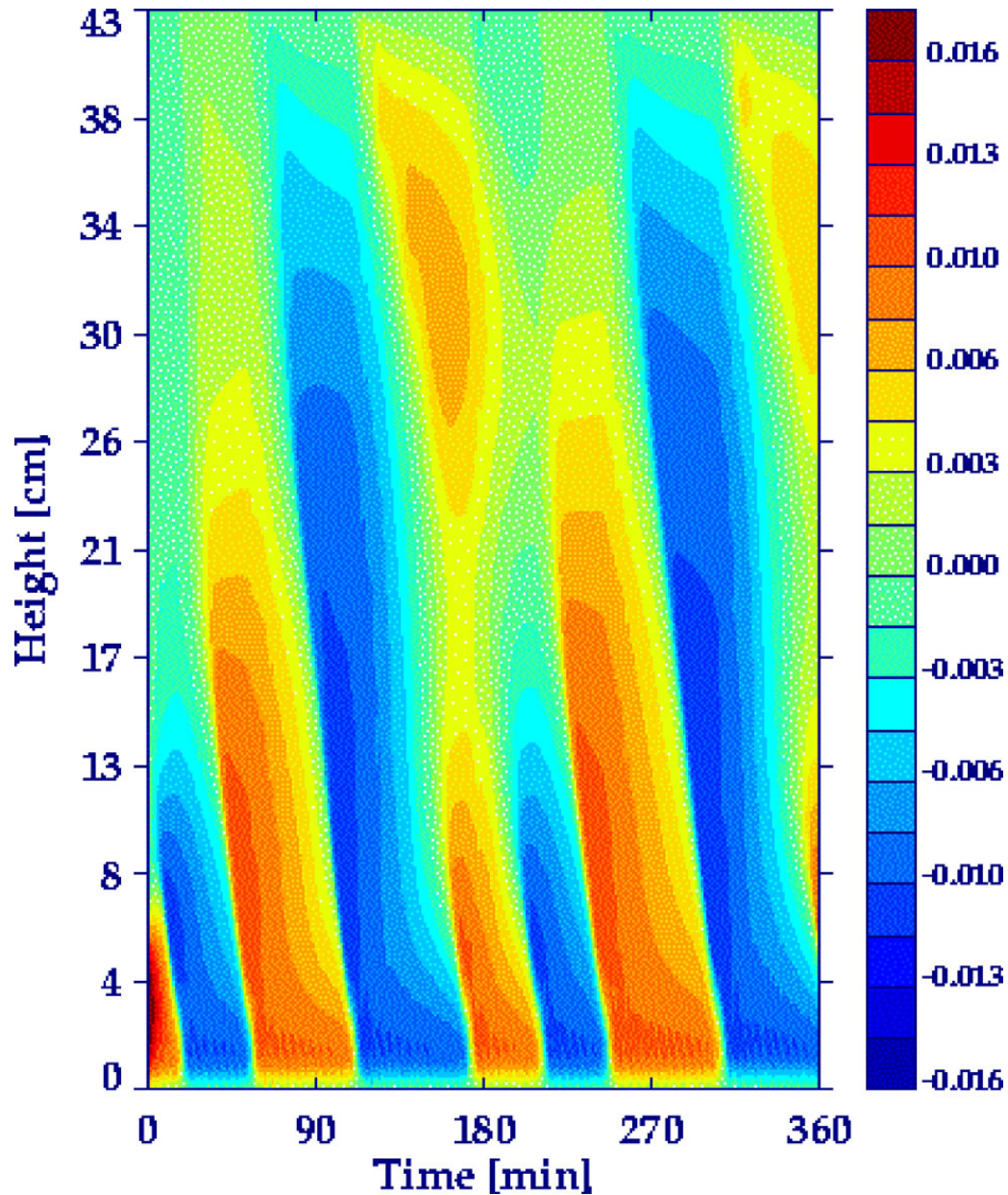


Schematic description of QBO laboratory analogue





Time – height cross
section of the mean
flow U
in a 2D Eulerian
simulation



Time – height cross
section of the mean
flow U
in a 2D
Semi-Lagrangian
simulation

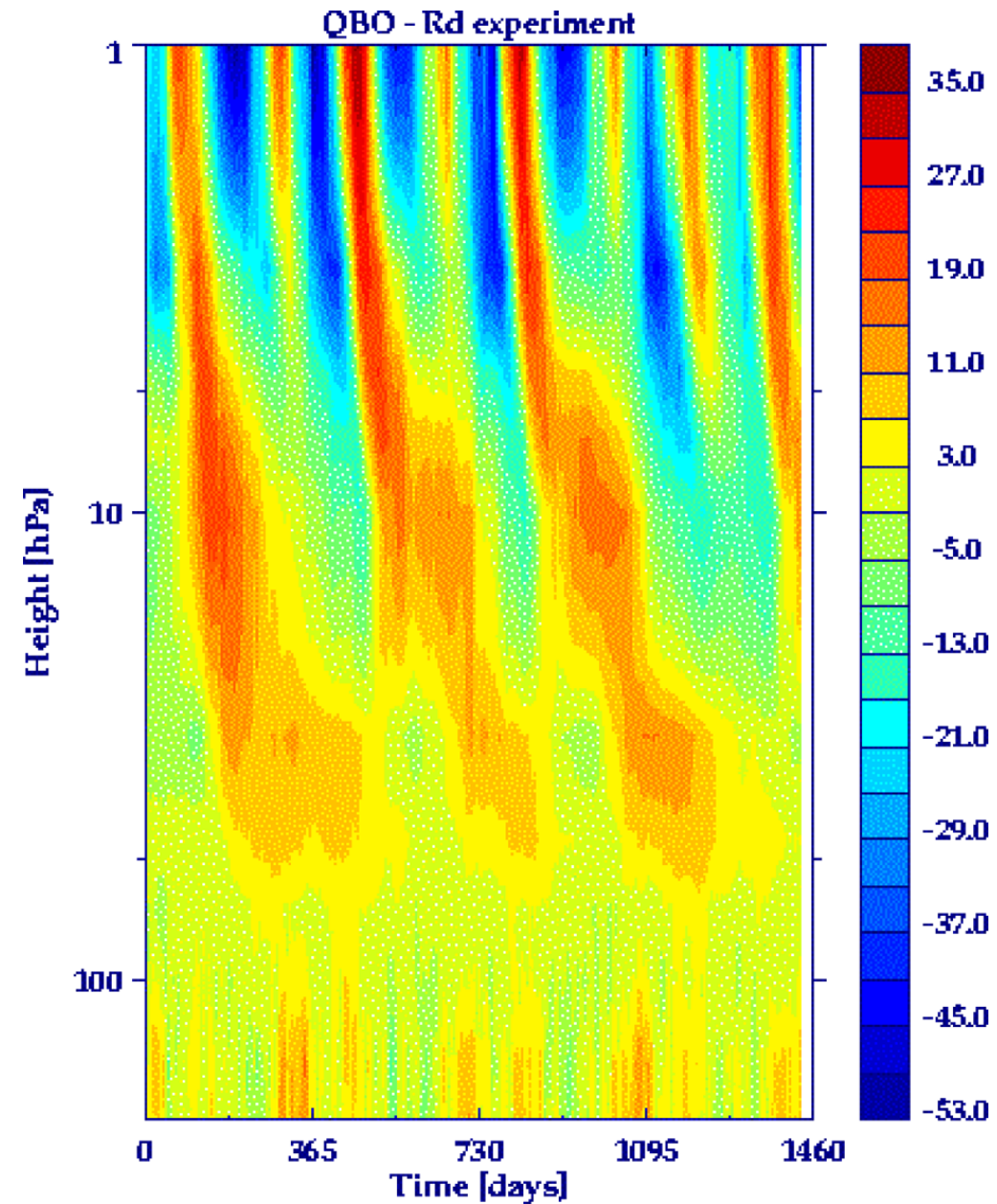
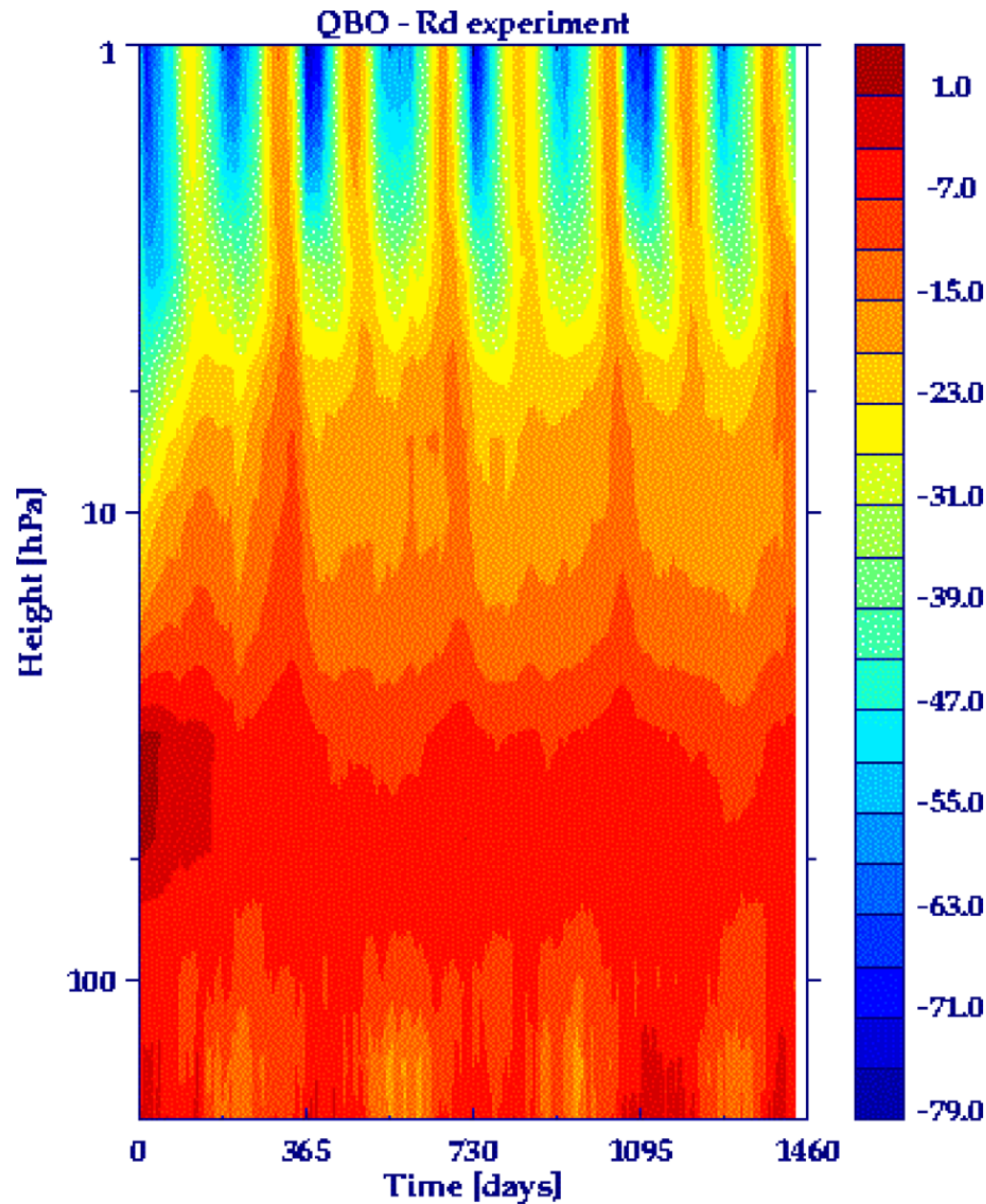
Numerical realizability

All these influence the numerical solution of the obtained wave dispersion, their dissipation and resulting zonal mean flow changes

- Sufficient resolution (*~10-15 points per wave, <5 no oscillation observed*)
- First or second order accurate (*rapid mean flow reversals with 1st order (alternating) scheme*)
- Accuracy of pressure solver (*only when $\varepsilon=10^{-3}$ mean flow change distorts*)
- Choice of advection scheme (*flux-form more accurate*)
- Explicit vs. implicit (*explicit is less accurate but recovers with ~2 times resolution*)
- Upper and lower boundaries (*only in 2D here due to wave reflection changing wave momentum flux, but an issue in atmospheric models*)



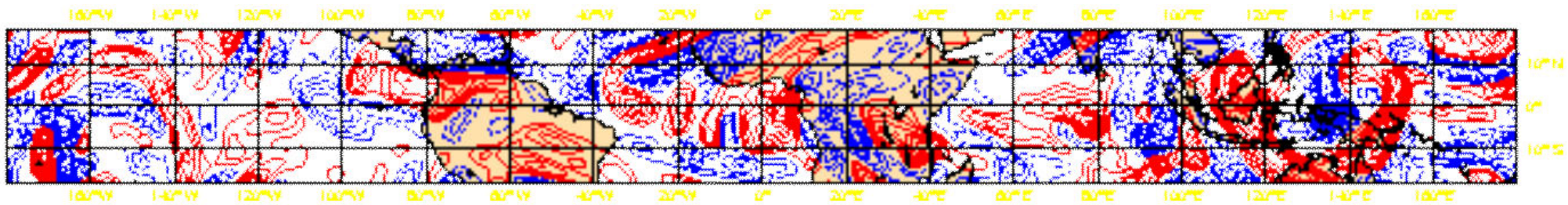
A QBO in IFS ?



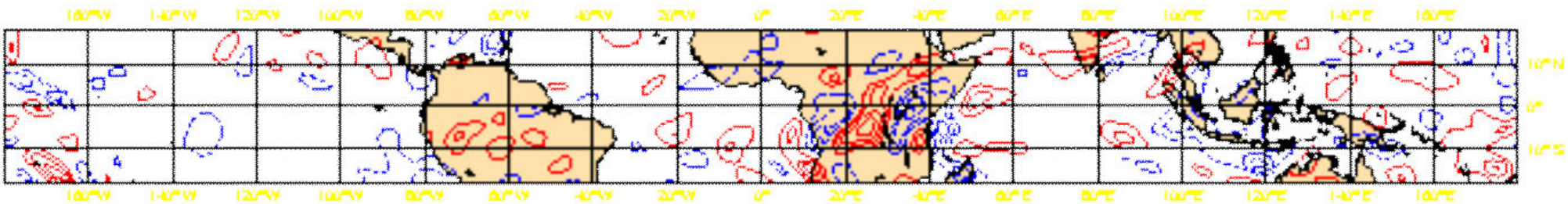
Numerically generated forcing !

Instantaneous horizontal velocity divergence at $\sim 100\text{hPa}$

No convection parameterization



Tiedke massflux scheme



T63 L91 IFS simulation over 4 years



Madden-Julian oscillation (MJO)

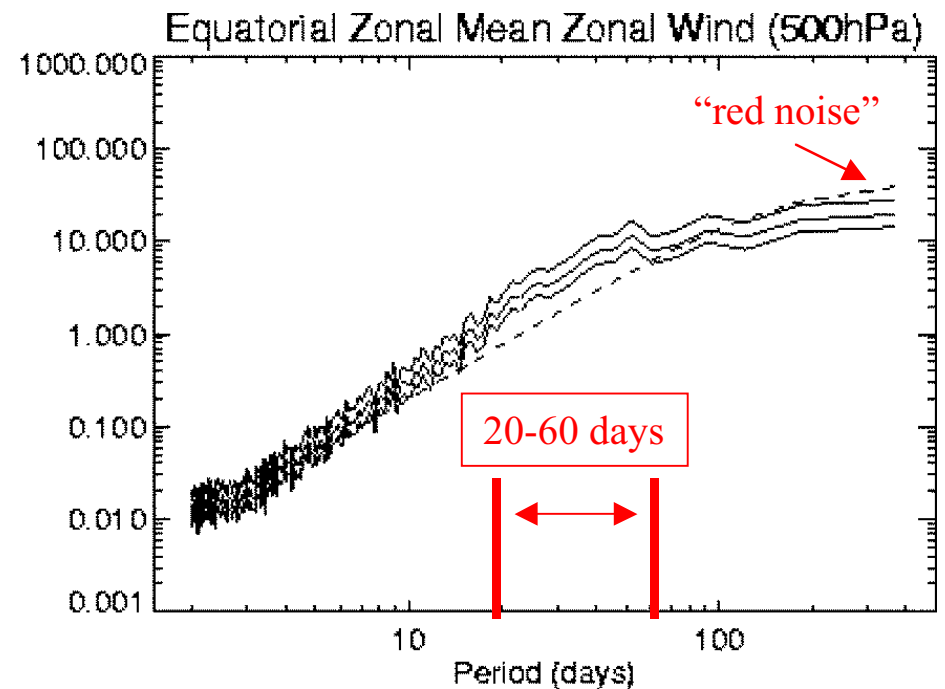
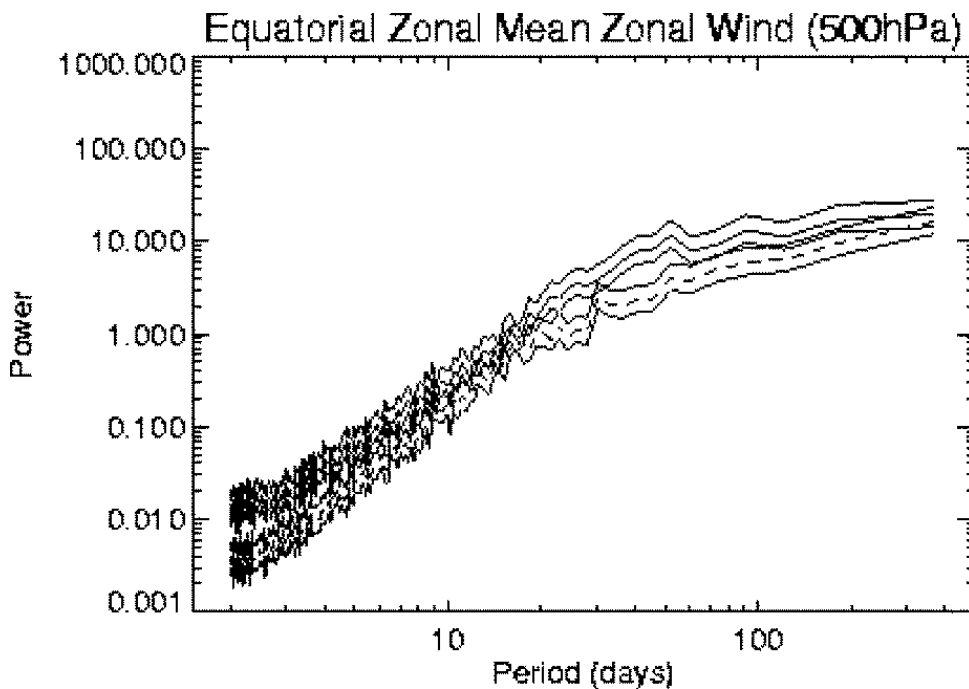
- The interference of horizontally propagating waves in the absence of dissipation can generate oscillatory zonal mean flow changes of the form:

$$\frac{\partial U}{\partial t} = -\frac{\partial}{\partial y} \langle u'v' \rangle_x .$$

Do we find zonal mean zonal flow changes with periods similar to the MJO ?



Madden-Julian oscillation (MJO)



35 years ERA40 – analysis (*solid line*)

35 years ERA40 – climate fc (*left plate dashed line*)

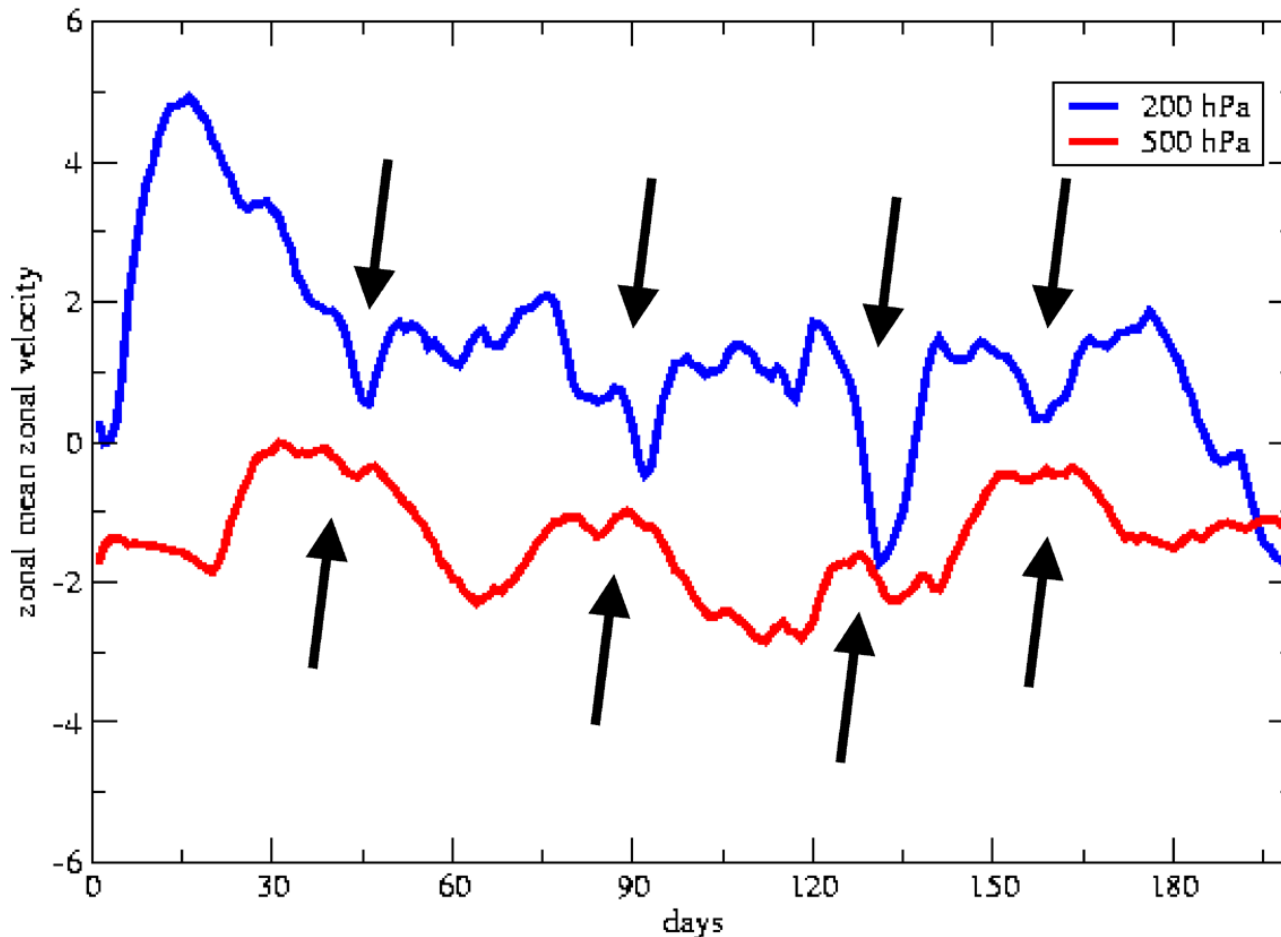
Fitted “red noise” (*right plate dashed line*)

(*T. Jung*)



MJO-like signal in T511 ?

T511 L60 zonal mean flow



The zonal mean zonal velocity exhibits a 30-50 day oscillation



Conclusions I

- There is a lot of intricate detail which cannot be deduced from experimental data alone, therefore there is a need for numerical simulations to complement laboratory studies
- The zonal mean flow oscillation in the tank is an entirely wave-interaction driven phenomena which exhibits wave interference, critical layer formation and subsequent wave breaking

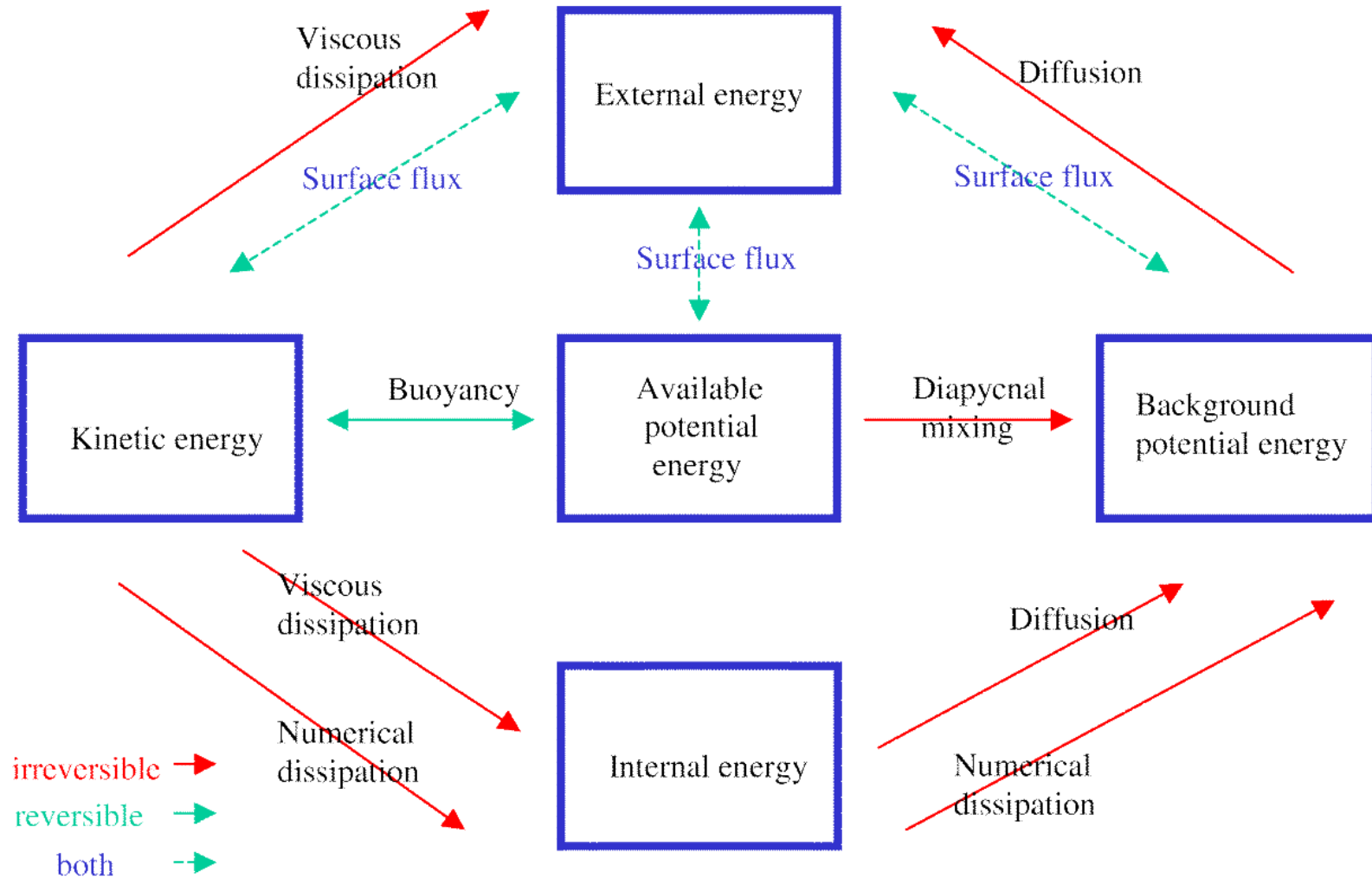


Conclusions II

- There is a long list of numerical influences on internal (gravity) wave dispersion and dissipation (boundaries, implicitness, accuracy!) and their distinction from physical phenomena may not be obvious
- Current and future high resolutions will resolve part of these internal wave processes but may not be accurate
- New demands on dynamical core test cases beyond Held-Suarez type simulations?
- Accuracy of parameterizations expressing the statistical effects of internal wave dissipation?



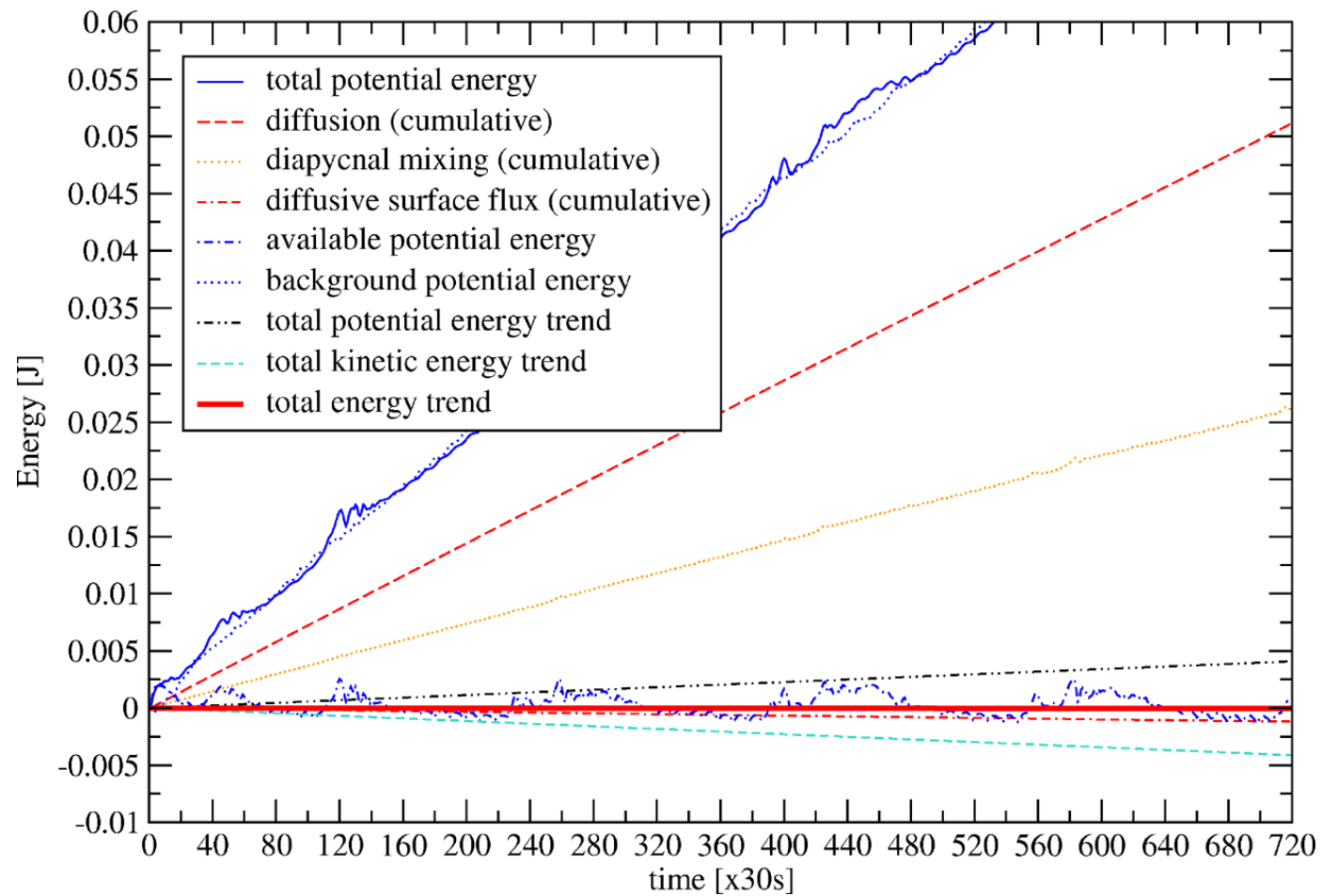
Energy



adapted from Winters et. Al. JFM 289 115-128 (1995)

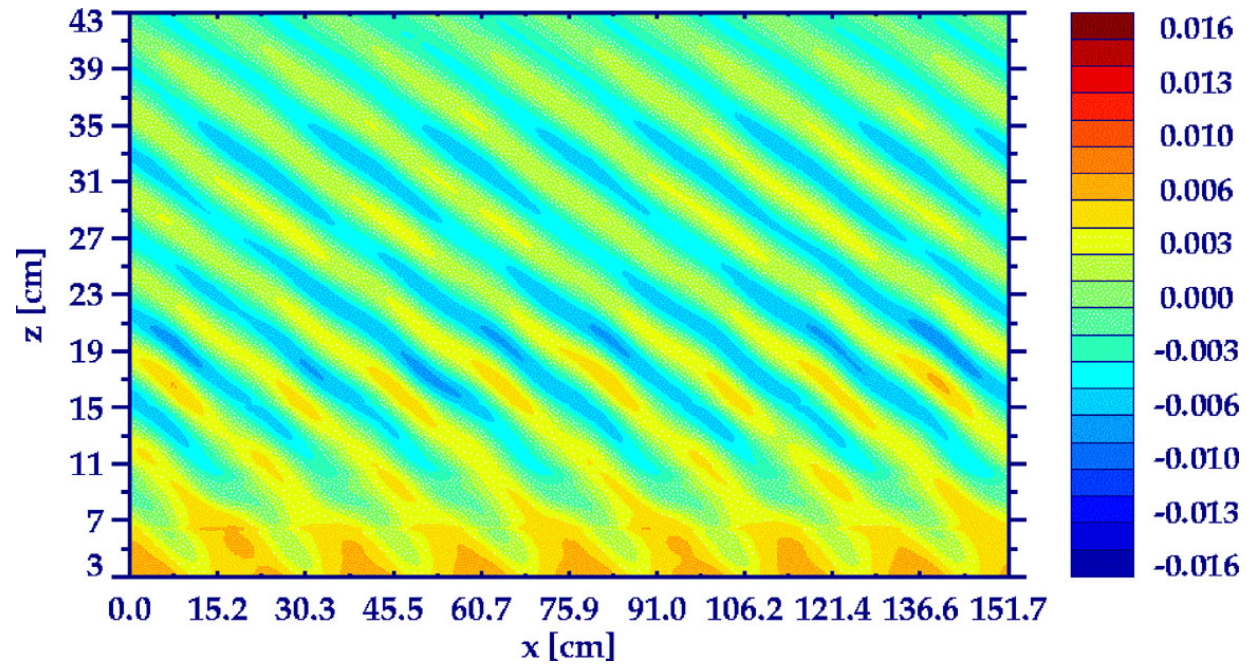


Energy



Reconstructed from $k=+8, 8 < m < 16$

T=24min



T=26min

